Lithuanian Journal of Physics, Vol. **58**, No. 1, pp. 116–125 (2018)

STUDY OF SURFACE ELECTRIC FIELD AND PHOTOCARRIER DYNAMICS IN InAs BY MEANS OF A MODIFIED DOUBLE-PUMP-PULSE TERAHERTZ EMISSION METHOD

I. Beleckaitė [a], L. Burakauskas [b], and R. Adomavičius [a]

[a] *Center for Physical Sciences and Technology, Saulėtekio 3, 10257 Vilnius, Lithuania*
[b] *Department of Physics, University of Oxford, Parks Rd, Oxford OX1 3PU, UK*
Email: ieva.beleckaite@ftmc.lt

Received 31 January 2018; accepted 22 March 2018

In this study we report the investigation of terahertz (THz) emission efficiency dynamics in p-type InAs using a double-pump-pulse (DPP) THz emission method. We also suggest a novel modification of the standard DPP method which allows us to measure the indirectly modulated THz pulse. The obtained results reveal that the first optical pulse increases the free carrier concentration and enhances the surface electric field. This field prevents perpendicular but improves parallel to the surface electric dipole formation after sample excitation with the second optical pulse. Our suggested method is shown to be a more precise and sensitive way to study electric fields and photocarrier dynamics in semiconductors after photoexcitation.

Keywords: photo-Dember effect, THz emission from semiconductors, InAs

PACS: 07.57.Hm, 78.47.D-, 78.47.J-

1. Introduction

During the last decades of the 20th century the technology of femtosecond lasers was highly improved. It opened a possibility to investigate physical processes that last less than 1 ps. For the first time in 1984 Auston et al. used a femtosecond laser for the registration of electromagnetic pulse with the duration of a few picoseconds transmitted through free space [1]. A few years later, in 1988, the first terahertz time-domain spectroscopy (THz TDS) system was presented [2]. Since then such systems have become more accomplished and have found many application areas. One of the most important components of the THz TDS system is a THz pulse emitter commonly activated with femtosecond laser pulses. THz emitters could be various semiconductors, their compounds and nanostructures or optoelectronic switches – semiconductors with metallic contacts that require external bias for operation. In order to gain a better understanding of THz generation mechanisms and create more effective THz emitters, various THz TDS system modifications are used. The main idea of one of rarely used modifications is to use two excitation pulses instead of one: the first pulse (pump) changes the carrier concentration and electric fields inside the semiconductor while the other (probe) arrives with a time delay and generates the THz pulse which reflects changes of the mentioned parameters. For the first time such double-pump-pulse terahertz emission (DPP THz) method was mentioned by Tanouchi el al. in 2002 [3]. They

investigated a low-temperature-grown GaAs (LT-GaAs) optoelectronic switch and reported the decrease in THz generation efficiency due to the screening of the bias electric field by generated photocarriers. The recovery of the THz signal was ascribed to the electron relaxation and recombination processes. A few years later Siebert et al. [4] basically repeated Tanouchi's results [3] but the authors elucidated the decrease of THz signal intensity due to changes in the voltage distribution in the biasing circuit. Later works by this group were intended to investigate the carrier recombination in LT-GaAs optoelectronic switches [5, 6]. Recently Murakami et al. [7] have expanded the potential of the DPP THz method by using a very sharply focused probe beam that allowed them to scan the whole area of an optoelectronic switch with a resolution of 1.5 μm. This upgraded DPP THz method was proved to be an excellent candidate for the investigation of electric field distribution dynamics in THz emitters after photoexcitation. In all previously cited works the electron drift was caused by an external bias which forced them to move parallel to the semiconductor surface. Speaking about the unbiased THz emitters, there is a greater variety of materials for samples. Optical reflection and DPP THz methods were compared in an article [8] where both of them were used for the investigation of LT-GaAs layers grown at different temperatures. While using the DPP THz method for the investigation of $CuInSe_2$ it was shown for the first time that the pump pulse could increase the THz emission efficiency [9]. The enhancement in the THz signal was also observed in GaAs nanowires (NWs) grown by the MOCVD method [10]. In addition, the DPP THz method was used to investigate the main principles of THz generation in InAs NWs [11]. The same technique but with a sharply focused probe beam was applied for the investigation of photovoltaic cells [12].

To our knowledge, there are no previous works where the temporal shape of the THz electric field transient ($E_{THz}(t)$) at different time delays between two excitation pulses has been investigated. In this work we show that $E_{THz}(t)$ strongly depends on the time delay between two optical excitation pulses. We reveal the main principles of the $E_{THz}(t)$ variation and suggest a more accurate method for THz emission DPP measurements. This method is applied to investigate a p-type InAs substrate that is known as one of the most efficient semiconductor-based THz surface emitters. It is shown that THz emission dynamics in InAs strongly depends on the polarization of an optical pulse that activates the THz generation process. From the obtained results we conclude that the sample excitation with the first optical pulse enhances its surface electric field. This field has a different effect upon the capability of the photocarriers created by the second excitation pulse to form parallel and perpendicular to the sample surface THz radiating electric dipoles.

2. Experimental details

In this article we report two types of double-pump-pulse excitation methods: standard (DPP) and our suggested modified (MDPP). All experiments were based on the experimental set-up that is shown in Fig. 1(a). Measurements have been performed using a Ti:sapphire oscillator generating 800 nm wavelength pulses at 76 MHz repetition rate, 6.5 nJ pulse energy and 150 fs pulse duration. The laser beam is divided into three parts: one part (≈20 mW) is directed towards a polarization sensitive GaAs THz detector (*Teravil Ltd*) for THz transient measurement; the other part is directed at the sample for THz pulse generation (the so-called Probe beam); the last part is also directed towards the sample for the generation of free carriers (Pump beam). In order to change Pump and Probe beam polarization, half-wave plates were used. During the DPP experiment the Pump Delay Line is fixed at the desirable time delay between the Pump and Probe pulses while the Detector Delay Line is used to coherently scan a temporal shape of the THz signal. The detected signal is analysed with a lock-in amplifier and transferred to the computer.

3. Results and discussion

The THz pulse dependence on the time delay between optical Pump and Probe pulses (Δt) measured with the standard DPP method (Fig. 1(b)) is shown in Fig. 2. The positive time delay ($\Delta t > 0$) means that the optical Pump pulse reaches the sample surface before the Probe pulse, and the negative time delay ($\Delta t < 0$) means

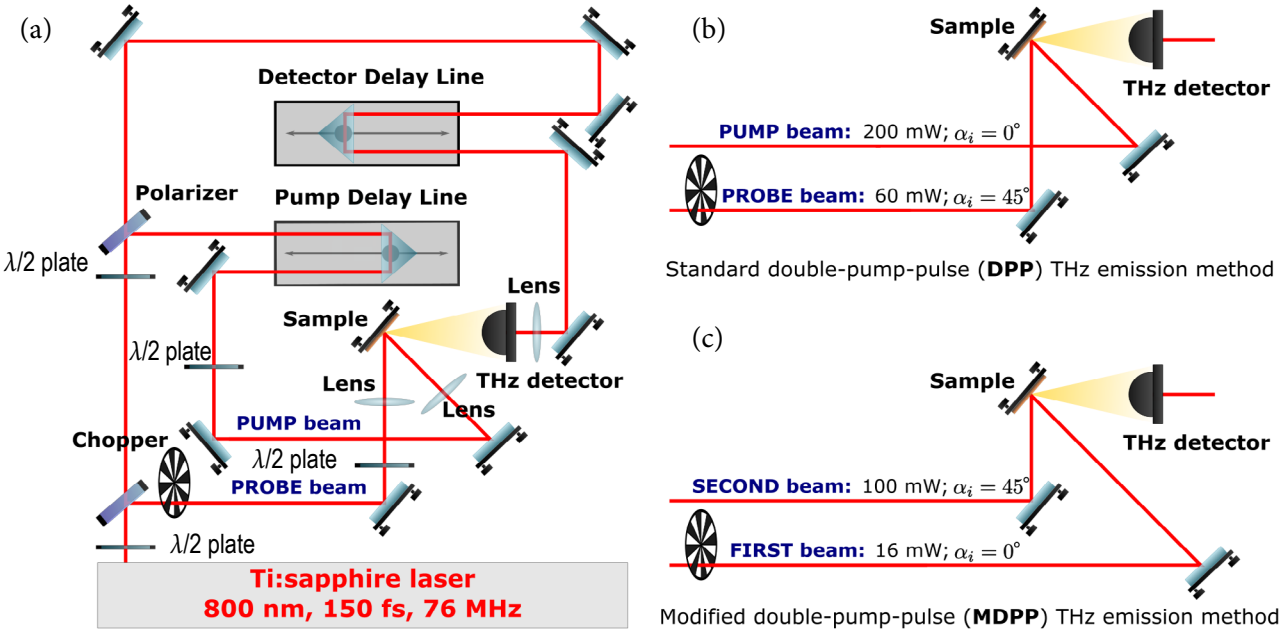

Fig. 1. Standard double-pump-pulse terahertz emission set-up. (a) Experimental set-up in general. (b) Standard double-pump-pulse terahertz emission method. (c) Modified double pump-pulse terahertz emission method.

that the Probe pulse comes before the Pump. In Fig. 2(a) it is possible to see a single THz pulse at different positive Δt. Generally speaking, both Pump and Probe pulses generate a THz pulse, but as the Probe beam is mechanically chopped due to the condition of synchronous detection, only the THz pulse generated by the Probe beam should be measured. Indeed, only the THz pulse generated by the Probe pulse is visible in Fig. 2(a). In this case the Pump beam only changes the conditions of the THz pulse generation. This effect is inert, thus with increasing Δt the registered THz pulse is more and more affected: the Pump pulse reduces the efficiency of THz generation. This is a typical result of the standard DPP THz measurement discussed in the previous works. In contrast,

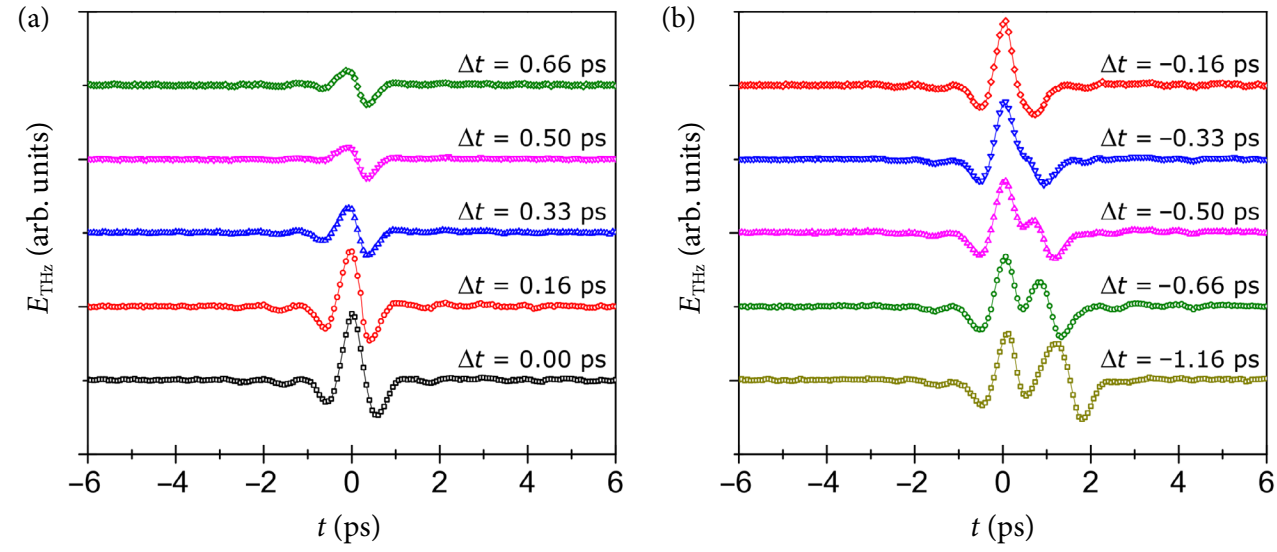

Fig. 2. THz pulse dependence on the positive (a) and the negative (b) time delay between optical Pump and Probe pulses. For positive time delays only the directly modulated THz pulse could be seen while for negative time delays both directly and indirectly modulated THz pulses are visible.

for negative Δt values the structure of the registered THz signal becomes more complicated (Fig. 2(b)). Overall, two kinds of THz pulses can be seen in Fig. 2: the first one is visible at all time delays and has a fixed position in the time scale; the second occurs only when the optical Probe pulse reaches the sample before the Pump pulse. The second pulse position in the time scale corresponds to the Δt, which suggests that we have the THz pulse generated by the Pump pulse. However, as mentioned before, the Pump beam is not mechanically chopped and due to the conditions of synchronous detection the THz pulse generated by the Pump pulse should not be registered. Nevertheless, a deeper analysis suggests that the generation of THz radiation with the Pump pulse is indirectly modulated. At negative time delays, when the Probe pulse reaches the sample before the Pump pulse, it creates photocarriers with the frequency of a mechanical chopper and affects the THz generation process initiated by the Pump pulse. So, as a result, the indirectly modulated THz pulse generated by the optical Pump pulse could be registered. Hence during the experiment we register the THz pulse generated by the Probe pulse and the indirectly modulated THz pulse corresponding to the difference in the THz emission generated by the Pump pulse due to the photocarriers created by the Probe pulse (the upper (green online) curve in Fig. 3). In comparison, the lower (red online) curve in Fig. 3 represents the same difference in THz generation but measured in a different way. Here the Pump pulse is chopped and the THz pulse measured with and without the additional excitation with the Probe pulse. Then both THz signals are subtracted from each other resulting in the difference in THz emission initiated by the Pump pulse due to the Probe pulse induced generation of the photocarriers. It is important to note that the position in the time scale of the indirectly modulated THz pulse in Fig. 2(b) is shifting during the experiment because the position of the Pump Delay Line is changing (Fig. 1).

It is obvious that the THz pulse registered due to the indirect modulation unavoidably affects dynamics measured by the traditional DPP THz method. When the Probe pulse arrives at the sample a few picoseconds earlier than the Pump pulse, the directly and indirectly modulated THz pulses are separated in the time scale (Fig. 4(a)). When

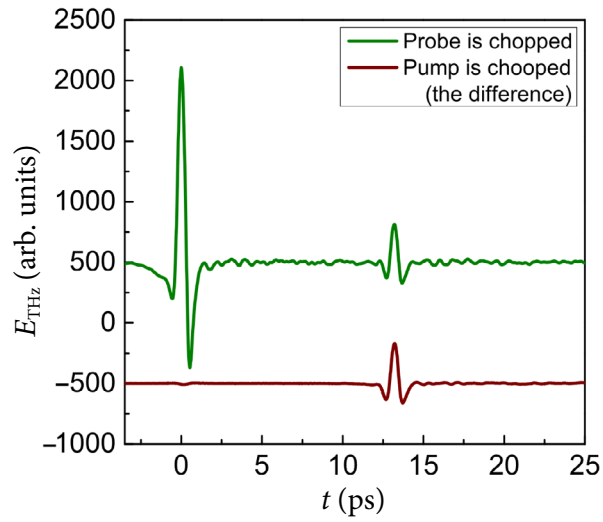

Fig. 3. THz pulses measured with different chopper positions at the time delay Δt = –13 ps. The upper (green online) curve represents the THz signal measured when the Probe beam is chopped. The lower (red) curve shows the difference in the THz signal with and without the Probe when the Pump beam is chopped.

the delay Δt approaches subpicosecond values, those two pulses overlap (Fig. 4(b)) and this pulse interference may seem like an increased THz pulse generated by the Probe laser pulse. Meanwhile, the Pump pulse reaching the semiconductor surface 0.5 ps later than the Probe pulse cannot affect the THz pulse generation process. Nevertheless, the indirectly modulated THz pulse is unique as it requires both Pump and Probe optical pulses for detection: if one of the pulses is blocked, this THz pulse vanishes. In addition, indirectly modulated THz pulse measurements at different Δt makes it possible to observe changes in the THz pulse generated due to the optically excited photocarrier relaxation.

The main idea of this work is to use indirectly modulated THz pulses for the investigation of THz generation dynamics. For this purpose, the set-up in Fig. 1(b) was modified to Fig. 1(c) as follows. The lower intensity mechanically chopped optical beam is directed perpendicular to the sample surface (the incidence angle equals 0°), while the higher intensity optical beam impinges on the sample surface at the 45° incidence angle. In order to detect the indirectly modulated THz pulse, the chopped optical pulse must be the first to reach the sample surface; therefore this pulse will be called the First pulse and the other will be called

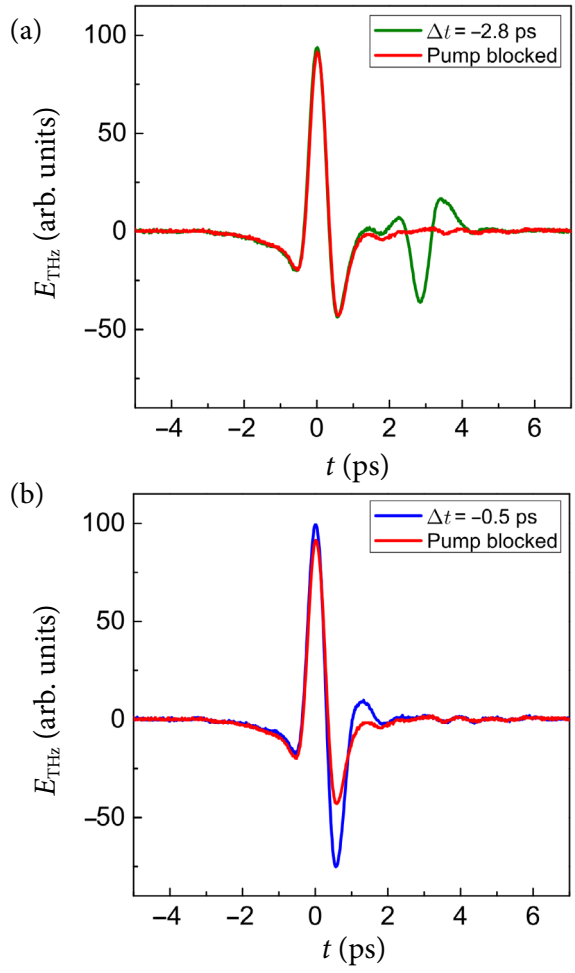

Fig. 4. Directly and indirectly modulated THz signals measured at different negative time delays (Δt = –2.8 ps (a) and Δt = –0.5 ps (b)). The repeating in (a) and (b) (red online) curve represents the directly modulated THz pulse created by the Probe pulse when the Pump pulse is blocked, the other (green online) curve in (a) shows the directly and indirectly modulated pulses separated in time and the other (blue online) curve in (b) presents the interaction of directly and indirectly modulated THz pulses that might be mistaken as enhancement of the Probe generated THz pulse.

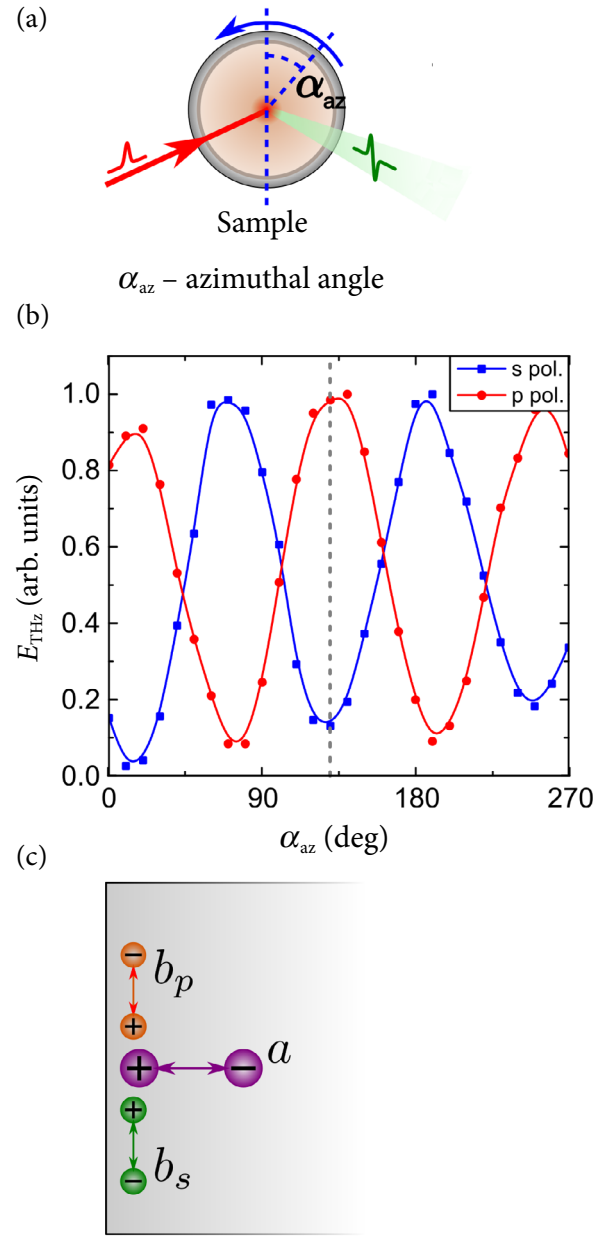

Fig. 5. (a) Schematic illustration of the THz emission efficiency dependence on an azimuthal angle measurement. The sample is rotating around the normal to the surface. (b) THz pulse amplitude dependence on an azimuthal angle for the s-polarized and the p-polarized optical pulse. (c) Schematic illustration of the electric dipoles formed in the sample after photoexcitation at an azimuthal angle ≈130°. There a corresponds to the perpendicular electric dipole while b_p and b_s to the parallel dipole excited with p or s light polarization.

the Second pulse. Before the DPP THz experiments the THz emission efficiency dependence on an azimuthal angle (Fig. 5(a)) in p type InAs (p-InAs) was measured using only the Second optical pulse: the First pulse was blocked and the chopper was moved to modulate the p-polarized Second pulse (the (red) curve with dots in Fig. 5(b)). The azimuthal angle for the maximum THz emission efficiency was determined and fixed for subsequent measurements (the dotted line in Fig. 5(b)). In Fig. 6(a, b) indirectly modulated THz pulses at different time delays between two optical excitation pulses are shown. THz pulse amplitudes (peak-to-valley) of these pulses are summarized in Fig. 6(c).

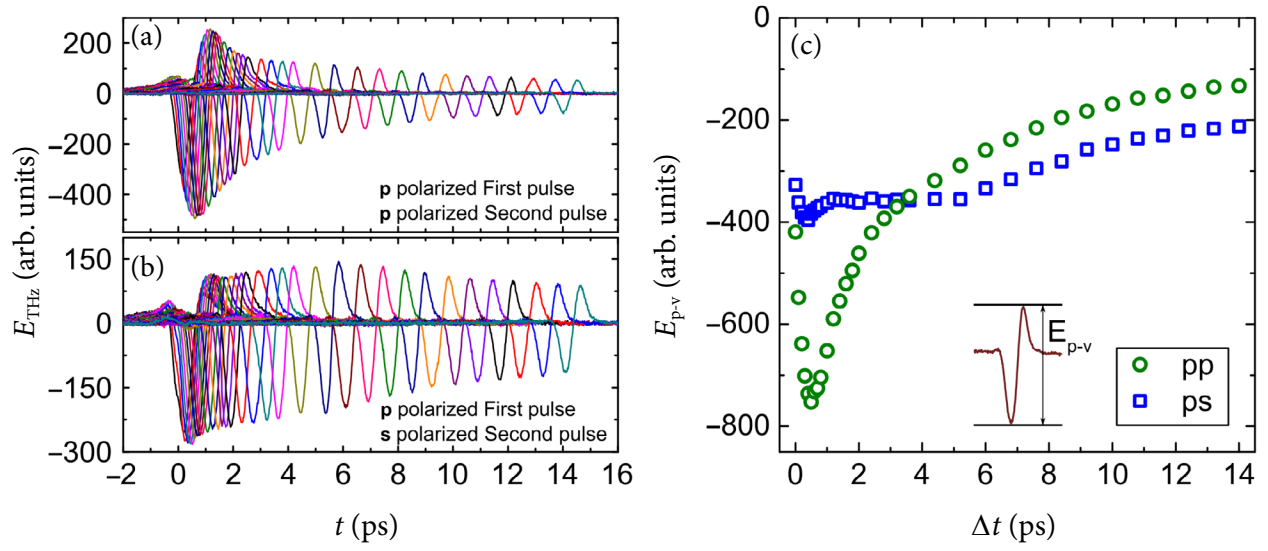

Fig. 6. Indirectly modulated THz pulses measured at different time delays for the p-polarized (a) and the s-polarized (b) Second pulse. The First pulse was always p-polarized. (c) The summarized THz pulse amplitudes (peak-to-valley) of these THz pulses.

The obtained curves show the influence of the First optical pulse to the THz generation process initiated by the Second pulse. It could be seen from the figure that THz generation properties strongly depend on the polarization of the Second pulse. It is worth mentioning that such dependence was not observed in other samples investigated by our introduced DPP THz method.

It should be noted that the ratio between optical pulse powers (the power of the Second pulse is a few times larger than that of the First pulse) is chosen intentionally. When the power of the First pulse exceeds 30 mW (that corresponds to 0.4 nJ energy and the concentration of photocarriers 3.4×10^{16} cm^{-3}), the shape of the measured kinetics changes dramatically. On the contrary, no such changes were observed for the increasing power of the Second pulse.

In order to understand the indirectly modulated THz pulse kinetics and its difference upon p and s optical polarization, it must be understood how the Second optical pulse generates the THz pulse. In all standard semiconductors photoexcited electrons and holes are separated in the surface electric field (field effect [13]) and/or compelled to move along the surface gradient at different velocities (photo-Dember effect [14]). Both effects result in the perpendicular to the sample surface electric dipole which emits THz radiation. It is also possible that the parallel to surface dipole will form. This could happen due to nonlinear optical effects [15] and most importantly due to anisotropic photocurrent effects [16] that are very important for narrow band-gap semiconductors (like InAs). In InAs electrons with high excess energy are created upon the excitation of 800 nm wavelength laser radiation. The motion of such electrons in the strong surface electric field leads to the formation of a parallel to the surface electric dipole due to the non-parabolicity [16] and non-sphericity [17] of the conduction band. When we rotate a sample around the normal to the surface, strength and orientation of the parallel electric dipole changes thus determining the THz emission efficiency dependence on an azimuthal angle. The orientation of the THz radiating electric dipole depends on the polarization of the excitation beam. It could be seen from the measured azimuthal dependences that under the p-polarized and s-polarized excitation the electric dipoles parallel to the surface are oriented in opposite directions (Fig. 5(c)). The THz emission from perpendicular to the surface electric dipole is supposed to remain constant. Then the registered THz radiation could be determined as the sum of the two components: $a + b_p$ and $a - b_s$. There a corresponds to the perpendicular electric dipole radiation, while b_p and b_s to the radiation of a parallel dipole excited

by p or s light polarization, respectively. Under the assumption that all the abovementioned electric dipoles always radiate the same form of THz pulses, the curves in Fig. 6(c) could be expected to be proportional to the $a + b_p$ and $a - b_s$ (here a, b_p, b_s are functions of the time delay Δt). Then the difference of these curves will be proportional to the $b_p + b_s$, while the sum could be described as $2a + b_p - b_s \approx 2a$ (we assume that $b_p \approx b_s$). It is obvious that the difference (sum) of the dependences in Fig. 6(c) describes the change in the THz radiation from the parallel (perpendicular) to the surface electric dipole initiated by the Second pulse and induced by the photocarriers excited by the First pulse.

The sum and difference of the curves in Fig. 6(c) is shown in Fig. 7. It should be noted that the results in Fig. 6(c) mean that the First pulse always reduces the THz pulse generated by the Second pulse. However, from the difference of the mentioned curves it could be seen that the THz emission from the parallel to the surface electric dipole is enhanced for the time interval of 3 ps after the surface excitation with the First pulse. To verify that the THz emission enhancement is real, measurements for the s-polarized THz electric field were performed. Many semiconductors form only a very weak parallel to the surface electric dipole and no s-polarized THz pulse could be detected. That is why usually polarization sensitive THz detectors are oriented to detect the p-polarized THz radiation. However, the (111) crystallographic orientation InAs emits a strong enough s-polarized THz pulse. It is important to mention that the perpendicular to the surface electric dipole has no influence over the s-polarized THz radiation. Figure 8(a) shows the indirectly modulated s-polarized THz pulse dynamics. To confirm the nature of the jump between positive and negative values, the chopper was moved to modulate the Second pulse. The bubble (blue) curves in Fig. 8(b) represent THz pulses when the First pulse is blocked, the dot (red) curves represent the results of the THz generation process affected by the First pulse. The results shown in Fig. 8(b) confirm that the THz emission efficiency can be enhanced using the additional excitation of the semiconductor surface. However, in our case this statement is true only for the parallel to the surface THz radiating electric dipole.

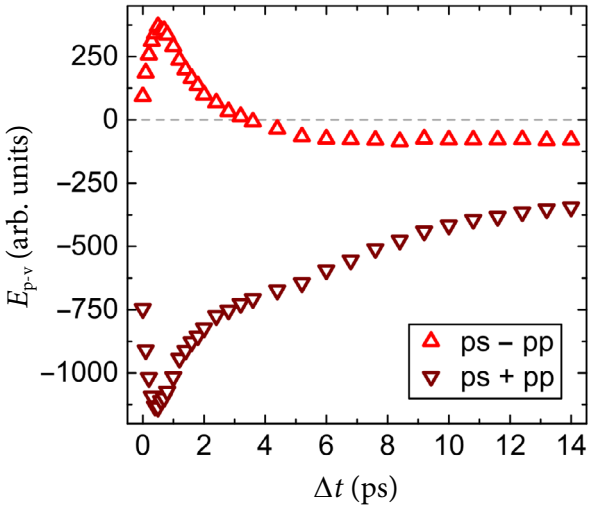

Fig. 7. Sum and difference of the curves shown in Fig. 6(c). The difference (sum) describes THz radiation from the parallel (perpendicular) to the surface electric dipole created by the Second pulse and modulated by the photocarriers excited by the First pulse.

The obtained results could be explained in terms of the two-kind influence of the photocarriers on the THz generation process. After the photoexcitation with the First pulse carrier motion is determined by the gradient and surface electric field. Within a few picoseconds after excitation, the surface electric field becomes stronger due to the carrier diffusion that is a dominant process at the beginning [18]. Then the motion of photocarriers created by the Second pulse is mostly controlled by the enhanced surface electric field. A stronger field obstructs the diffusion of new photocarriers [19] but stimulates the formation of the parallel to the surface electric dipole. Nevertheless, it must be kept in mind that photocarriers always affect THz generation even if they do not change the surface electric field. While photocarriers created by the Second pulse form an electric dipole, the photocarriers created by the First pulse move in the electric field of this dipole and create their own dipole of the opposite orientation. It means that free photocarriers always limit the THz generation process regardless of the THz radiating electric dipole orientation. It must be noted that the free carrier influence on the THz generation strongly depends on their energy relaxation time. Thus in narrow band-gap semiconductors the THz generation is almost unaffected due to

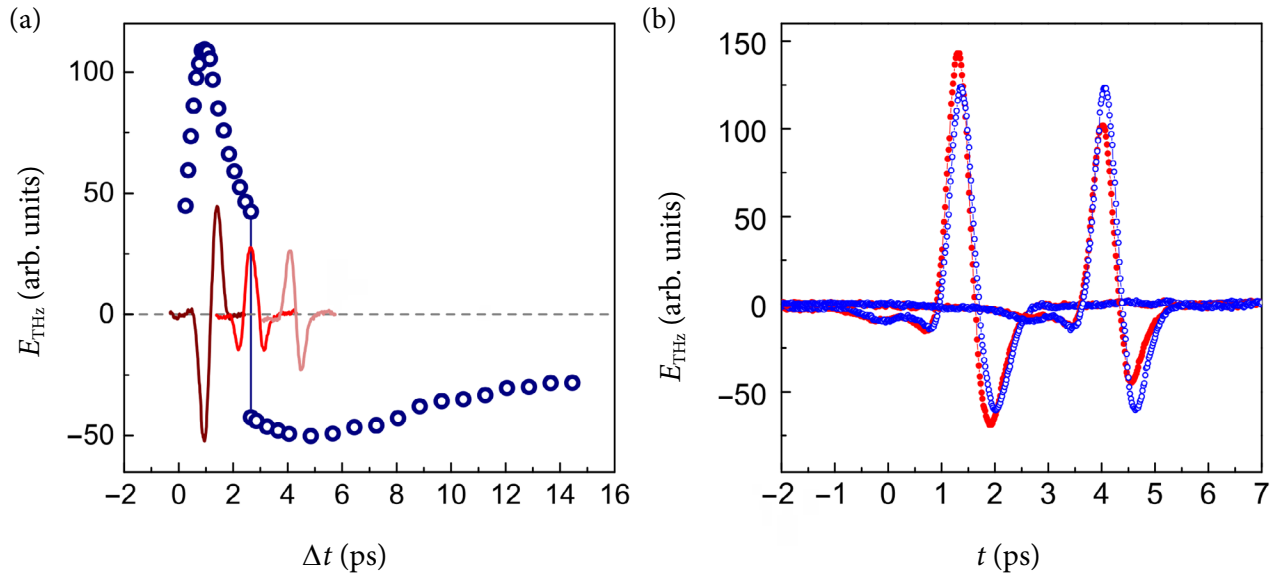

Fig. 8. (a) Bubble (blue online) dots represent the indirectly modulated s-polarized THz pulse amplitude (peak-to-valley) dynamics. Curves (red online) show the corresponding THz pulses. (b) Bubble (blue online) curves represent THz pulses when the First pulse is blocked, dot (red online) curves show the results of the THz generation process affected by the First pulse. THz emission enhancement (at t = 1.4 ps) and attenuation (at t = 4 ps) could be seen.

a relatively large electron mass during the first few picoseconds after the photoexcitation [20].

We have suggested the essential modification of the standard DPP THz emission method and showed its functionality by investigating p-type InAs. In the MDPP method registered THz pulse parameters depend on the versatile contribution of both optical pulses. For instance, the indirectly modulated THz pulse amplitude is proportional to the surface electric field alteration induced by the First pulse. This property allows us to investigate not only the electric field screening dynamics but also the dynamics of the Dember potential that is significant for the THz generation. Furthermore, our suggested MDPP method opens the possibility to investigate semiconductors at low excitation conditions when it is easier to separate physical mechanisms responsible for the THz generation. Additionally, the measurement of the indirectly modulated THz pulse is a novel promising contact-free method to investigate electric properties of photocarriers. Moreover, the time resolution of this method is a few hundreds of femtoseconds (the time period required for THz pulse generation), therefore rapid processes, for example, the ballistic electron transport dynamics, could be measured.

4. Conclusions

In conclusion, we have investigated the THz emission efficiency dynamics in InAs after sample excitation with the femtosecond optical pulse by means of the DPP method. Moreover, we have suggested a modification of the standard DPP method – whose main goal is to measure the indirectly modulated THz pulse. The analysis of the temporal shape of this pulse opens the possibility for a more precise and sensitive registration of changes in a semiconductor. We have shown that InAs excitation with the First pulse increases the free carrier concentration and enhances the surface electric field. This field prevents perpendicular but improves parallel to the surface electric dipole formation after sample excitation with the Second pulse. Free carriers screen both types of the dipole although their influence becomes noticeable over a few picoseconds after the excitation when the electron energy relaxation process is completed.

References

[1] D.H. Auston, K.P. Cheung, and P.R. Smith, Picosecond photoconducting Hertzian dipoles,

Appl. Phys. Lett. **45**(3), 284 (1984), https://doi.org/10.1063/1.95174

[2] P.R. Smith, D.H. Auston, and M.C. Nuss, Subpicosecond photoconducting dipole antennas, IEEE J. Quantum Electron. **24**(1), 255 (1988), https://doi.org/10.1109/3.121

[3] M. Tonouchi, N. Kawasaki, T. Yoshimura, H. Wald, and P. Seidel, Pump and probe terahertz generation study of ultrafast carrier dynamics in low-temperature grown-GaAs, Jpn. J. Appl. Phys. **41**(6B), L706 (2002), https://doi.org/10.1143/jjap.41.l706

[4] K.J. Siebert, A. Lisauskas, T. Löffler, and H.G. Roskos, Field screening in low-temperature-grown GaAs photoconductive antennas, Jpn. J. Appl. Phys. **43**(3), 1038 (2004), https://doi.org/10.1143/jjap.43.1038

[5] G.C. Loata, T. Löffler, and H.G. Roskos, Evidence for long-living charge carriers in electrically biased low-temperature-grown GaAs photoconductive switches, Appl. Phys. Lett. **90**(5), 052101 (2007), https://doi.org/10.1063/1.2436719

[6] G.C. Loata, M.D. Thomson, T. Löffler, and H.G. Roskos, Radiation field screening in photoconductive antennae studied via pulsed terahertz emission spectroscopy, Appl. Phys. Lett. **91**(23), 232506 (2007), https://doi.org/10.1063/1.2823590

[7] H. Murakami, S. Fujiwara, I. Kawayama, and M. Tonouchi, Study of photoexcited-carrier dynamics in GaAs photoconductive switches using dynamic terahertz emission microscopy, Photon. Res. **4**(3), A9 (2016), https://doi.org/10.1364/prj.4.0000a9

[8] V.K. Mag-usara, S. Funkner, G. Niehues, E.A. Prieto, M.H. Balgos, A. Somintac, E. Estacio, A. Salvador, K. Yamamoto, M. Hase, and M. Tani, Low temperature-grown GaAs carrier lifetime evaluation by double optical pump terahertz time-domain emission spectroscopy, Opt. Express **24**(23), 26175 (2016), https://doi.org/10.1364/oe.24.026175

[9] R. Adomavičius, A. Krotkus, J. Kois, S. Bereznev, and E. Mellikov, Terahertz radiation from non-stoichiometric $CuInSe_2$ films excited by femtosecond laser pulses, Appl. Phys. Lett. **87**(19), 191104 (2005), https://doi.org/10.1063/1.2126796

[10] V.N. Trukhin, A.D. Buravlev, V. Dhaka, G.E. Cirlin, I.A. Mustafin, M.A. Kaliteevski, H. Lipsanen, and Y.B. Samsonenko, Ultrafast carrier dynamics in GaAs nanowires, Lith. J. Phys. **54**(1), 41 (2014), https://doi.org/10.3952/physics.v54i1.2844

[11] A. Arlauskas, J. Treu, K. Saller, I. Beleckaitė, G. Koblmüller, and A. Krotkus, Strong terahertz emission and its origin from catalyst-free InAs nanowire arrays, Nano Lett. **14**(3), 1508 (2014), https://doi.org/10.1021/nl404737r

[12] H. Nakanishi, A. Ito, K. Takayama, I. Kawayama, H. Murakami, and M. Tonouchi, Visualization of photoexcited carrier responses in a solar cell using optical pump–terahertz emission probe technique, J. Infrared Millim. Terahertz Waves **37**(5), 498–506 (2015), https://doi.org/10.1007/s10762-015-0233-x

[13] X.-C. Zhang, B.B. Hu, J.T. Darrow, and D.H. Auston, Generation of femtosecond electromagnetic pulses from semiconductor surfaces, Appl. Phys. Lett. **56**(11), 1011 (1990), https://doi.org/10.1063/1.102601

[14] T. Dekorsy, H. Auer, H.J. Bakker, H.G. Roskos, and H. Kurz, THz electromagnetic emission by coherent infrared-active phonons, Phys. Rev. B **53**(7), 4005 (1996), https://doi.org/10.1103/PhysRevB.53.4005

[15] M. Reid, I.V. Cravetchi, and R. Fedosejevs, Terahertz radiation and second-harmonic generation from InAs: bulk versus surface electric-field-induced contributions, Phys. Rev. B **72**(3), 035201(2005), https://doi.org/10.1103/PhysRevB.72.035201

[16] V.L. Malevich, P.A. Ziaziulia, R. Adomavičius, A. Krotkus, Y.V. Malevich, Terahertz emission from cubic semiconductor induced by a transient anisotropic photocurrent, J. Appl. Phys. **112**(7), 073115 (2012), https://doi.org/10.1063/1.4758181

[17] P. Cicėnas, A. Geižutis, V.L. Malevich, and A. Krotkus, Terahertz radiation from an InAs surface due to lateral photocurrent transients, Opt. Lett. **40**(22), 5164 (2015), https://doi.org/10.1364/ol.40.005164

[18] V.M. Polyakov and F. Schwierz, Influence of band structure and intrinsic carrier concentration on the THz surface emission from InN and InAs,

Semicond. Sci. Technol. **22**(9), 1016 (2007), https://doi.org/10.1088/0268-1242/22/9/007

[19] A. Krotkus, R. Adomavičius, G. Molis, and V.L. Malevich, Terahertz emission from InAs surfaces excited by femtosecond laser pulses, J. Nanoelectron. Optoe. **2**(1), 108 (2007), https://doi.org/10.1166/jno.2007.011

[20] R. Adomavičius, R. Šustavičiūtė, and A. Krotkus, in: *Narrow Gap Semiconductors 2007*, eds. B. Murdin and S. Clowes (Springer, Dordrecht, 2008) pp. 41–43, https://doi.org/10.1007/978-1-4020-8425-6_10

InAs PAVIRŠINIO ELEKTRINIO LAUKO IR KRŪVININKŲ DINAMIKOS TYRIMAS MODIFIKUOTA DVIGUBO IMPULSINIO ŽADINIMO TERAHERCINĖS EMISIJOS METODIKA

I. Beleckaitė [a], L. Burakauskas [b], R. Adomavičius [a]

[a] *Fizinių ir technologijos mokslų centras, Vilnius, Lietuva*

[b] *Oksfordo universiteto Fizikos departamentas, Oksfordas, Jungtinė Karalystė*

Santrauka

Atlikome išsamią dvigubo žadinimo terahercinės emisijos metodo analizę, atskleidėme metodo trūkumus ir pasiūlėme, kaip patobulinti matavimo procedūrą. Taikant patobulintą metodiką ištirta terahercinės spinduliuotės generavimo dinamika p tipo InAs padėkle. Eksperimento metu registruotas terahercinis impulsas tiesiogiai atspindėjo pirmojo optinio impulso nulemtus pokyčius puslaidininkio paviršiuje. Prieita prie išvados, kad pirmąsias kelias pikosekundes po sužadinimo terahercinės spinduliuotės generavimo sąlygos labiausiai keičiasi dėl foto-Demberio efekto, o vėliau svarbesnis tampa ekranavimas šviesa sužadintais laisvaisiais krūvininkais. Eksperimento rezultatai parodė, kad terahercinės spinduliuotės generavimo dinamika labai priklauso nuo žadinančios šviesos poliarizacijos. Šis rezultatas paaiškinamas skirtinga elektrinio lauko pokyčių įtaka terahercinius impulsus spinduliuojančių elektrinių dipolių formavimuisi. InAs padėklo sužadinimas pirmuoju impulsu dėl foto-Demberio efekto sustiprina jo paviršinį elektrinį lauką. Šis laukas trukdo vėliau sužadintiems krūvininkams formuoti statmeną, bet padeda sudaryti lygiagretų paviršiui dipolį. Laisvieji krūvininkai ekranuoja bet kokio tipo dipolius, tačiau jų poveikis pasireiškia po kelių pikosekundžių, įvykus elektronų energijos relaksacijai.